Prototype of solar ground layer adaptive optics at the 1 m New Vacuum Solar Telescope

Lin Kong (孔 林)[1,2,3], Lanqiang Zhang (张兰强)[1,2,*], Lei Zhu (朱 磊)[1,2], Hua Bao (鲍 华)[1,2], Youming Guo (郭友明)[1,2], Xuejun Rao (饶学军)[1,2], Libo Zhong (钟立波)[1,2], and Changhui Rao (饶长辉)[1,2]

[1]*The Key Laboratory on Adaptive Optics, Chinese Academy of Sciences, Chengdu 610209, China*
[2]*The Laboratory on Adaptive Optics, Institute of Optics and Electronics, Chinese Academy of Sciences, Chengdu 610209, China*
[3]*University of Chinese Academy of Sciences, Beijing 100049, China*
**Corresponding author: lqzhang@ioe.ac.cn*

Received June 11, 2016; accepted August 19, 2016; posted online September 19, 2016

A prototype of a solar ground-layer adaptive optics (GLAO) system, which consists of a multi-direction correlating Shack–Hartmann wavefront sensor with 30 effective subapertures and about a 1 arcmin field of view (FoV) in each subaperture, a deformable mirror with 151 actuators conjugated to the telescope entrance pupil, and a custom-built real-time controller based on field-programmable gate array and multi-core digital signal processor (DSP), is implemented at the 1 m New Vacuum Solar Telescope at Fuxian Solar Observatory and saw its first light on January 12th, 2016. The on-sky observational results show that the solar image is apparently improved in the whole FoV over 1 arcmin with the GLAO correction.

OCIS codes: 010.1080, 110.1080.
doi: 10.3788/COL201614.100102.

Understanding the processes that generate and concentrate magnetic energy in the solar atmosphere is one of the most important challenges for solar physics. Adaptive optics (AO) is an indispensable technique in ground-based solar imaging that provides diffraction-limited resolution but has only a very small corrected field of view (FoV). In solar observation, the interesting active regions often extend to 1–2 arcmin[1].

Multi-conjugate adaptive optics (MCAO) is significantly considered as the most promising technique to increase the corrected FoV. The sun is an ideal target to perform MCAO, since solar surface structures such as sunspots and granulation can provide multiple "guide stars" in any configuration. The 0.76 m Dunn Solar Telescope (DST) took the lead in developing a solar MCAO experiment[2]. It consisted of a 5×5 subaperture multi-direction correlating Shack–Hartmann wavefront sensor (MD-SHWFS) with three guiding regions within the 1.25 arcmin full FoV and two deformable mirrors (DMs) with 97 actuators conjugated at the ground layer and 2.6 km and was developed in 2004. However, the experiment was unsuccessful. The 0.7 m Vacuum Tower Telescope showed their MCAO experiment in 2005[3], which contained a valid 6-subaperture MD-SHWFS with 19 subfields covering the full 1 arcmin and two DMs conjugated at the ground layer and 8–16 km. However, the result is not really good. MCAO was also developing at the 1.5 m GREGOR Solar Telescope[4] and the 1.6 m New Solar Telescope[5] currently. Until now, there is no routine operational solar MCAO in practice.

That fact that about 60% of the turbulence strength is concentrated in the first few kilometers above the telescope inspired the concept of ground-layer adaptive optics (GLAO)[6]. The ground layer (<500 m) contains 55%–65% of the turbulence during the daytime above the Big Bear Solar Observatory[7]. A GLAO system can be seen as a simplified MCAO system that is required to have several wavefront sensors to measure the wavefront perturbation introduced by the ground turbulent layer and a single DM conjugated to a low altitude to compensate for the ground turbulent layer. As opposed to the MCAO, it is important to emphasize that the goal of GLAO is not to attain a near-diffraction-limited correction, but to simply reduce and stabilize sight over a wide FoV. Rimmele *et al.*[8] developed a solar GLAO system at the DST in 2010. They used a WFS conjugated to the ground layer and averaged the three wavefront distortions in an FoV of $42'' \times 42''$. However, it was unsuccessful, because of the poor SHWFS sampling accuracy (at $2''$ per SHWFS detector pixel), which cannot provide an acceptable AO performance. Ren *et al.*[9] introduced two wavefront sensing methods for GLAO and implemented the large guide star (LGS herein) method at variable seeing conditions in the near-infrared (NIR) J- and H-bands. The SHWFS has 9×9 subapertures and the wavefront FOV is only $30'' \times 30''$. For the discrete guide (DGS herein) method, they only give the simulation result. In this Letter, we implement the GLAO system with the DGS method and achieve an apparent correction image in the visible band.

A number of attempts were also made to develop a solar AO system by the Institute of Optics and Electronics (IOE), Chinese Academy of Sciences, during the last fifteen years. A tilt-correction AO system was developed

for the 43 cm Solar Telescope of Nanjing University[10] in 2002. In 2008, a 37-element AO experimental prototype, which is the first solar AO system in China, was successfully installed for the 26 cm fine-structure solar telescope at Yunnan Astronomical Observatory and saw its first light in September 2009[11,12]. This prototype had been modified and tested at the 1 m New Vacuum Solar Telescope (NVST) of the Fuxian Solar Observatory (FSO) in 2011[13]. After that, we developed two generations of AO systems with 37-element low-order and 127-element high-order for the NVST[14,15]. In order to achieve a wider field, we developed a GLAO prototype system for the 1 m NVST. This system saw its first light on January 12th, 2016.

In this Letter, we first introduce an overview of the system, including the optical layout and parameters of the system, and then summarize the preliminary results from a recent GLAO observation run at the NVST and discuss future plans.

In 2010, the 1 m NVST was integrated and installed on the FSO, which is located on the northeast shore of Fuxian Lake, Yunnan, China. The telescope is based on a typical Gregory–Coudé design. The pure aperture of telescope is 985 mm, and the effective focal length before instruments is 45 m. The average seeing (Fried parameter, r_0) of the FSO obtained in the period from 1998 to 2000 was about 10 cm[16].

Figure 1 illustrates the optical layout of the GLAO experiment system, which is mounted after the Coudé focus of the telescope. Sunlight from the telescope is collimated to a suitable beam to feed into the tip tilt mirror (TTM) and then the DM, which is conjugated to the entrance pupil after flat mirror M1 and the off-axis parabolic mirror OAP1. The reimaging optics system, which consists of two off-axis parabolic mirrors OAP2 and OAP3, collimates the beam into a 16 mm aperture, and then the dichroic beam splitter BS1 divides the beam into two beams. One of the beam goes into the TiO band imaging subsystem, and the other beam is divided by beam splitter BS2 for MD-SHWFS and the corresponding tracking sensor.

The GLAO prototype system, which is based on a high-order AO system, contains a DM with 151 actuators conjugated to the telescope entrance pupil and a 30-subaperture MD-SHWFS with 5 subfields in each subaperture and a custom-built real-time controller based on field-programmable gate array (FPGA) and multi-core digital signal processor (DSP). In order to not affect the operation of the high-order AO system while also saving costs and space, we just install an MD-SHWFS for the

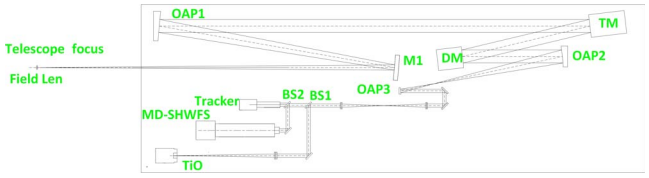

Fig. 1. Optical layout of the GLAO system. TM: tilt mirror.

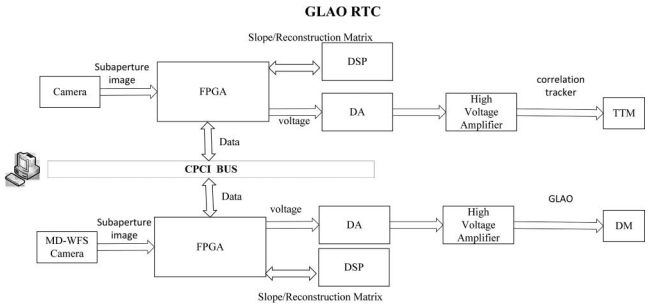

Fig. 2. Hardware scheme of real-time controller for the GLAO system.

first GLAO experiment. A new MD-SHWFS is considered now to match the 151-element DM based on a better camera with a larger target and faster frame rate. The real-time controller is composed of a fine tracking loop with a TTM and a GLAO correlation loop with a 151-actuator DM and a correlating MD-SHWFS based on the absolute difference square algorithm. In the fine tracking loop, the correlation tracker is the same as the high-order AO system, and the real-time controller of the GLAO system is shown in Fig. 2. The camera data were transferred to the FPGA, and then the FPGA processes the subaperture data to get the slopes with the absolute difference square algorithm when a subaperture row has been cached. All slopes are sent to the DSP by Serial RapidIO (SRIO) communication, and after the DSP finishes parabolic interpolation, matrix reconstruction, and control computation, the voltages are sent back to the FPGA. Then, the voltages are sent to a high-voltage amplifier by a DA converter to control the DM. The total computing delay is less than one clock period of the camera. The host PC is applied to display the image by a graphical user interface and to send parameters to the FPGA by a compact peripheral component interconnect (CPCI) bus.

Figure 3 shows the arrangements of the DM with 151 actuators and the subapertures of MD-SHWFS with 30 subapertures in the GLAO correction loop. The MD-SHWFS plays a very important role in the GLAO system. It can detect wavefront information from different directions at the same time and also has a larger FoV over 1 arcmin in each subaperture than a traditional SHWFS. Commonly, an SHWFS corresponds to a guide star. That

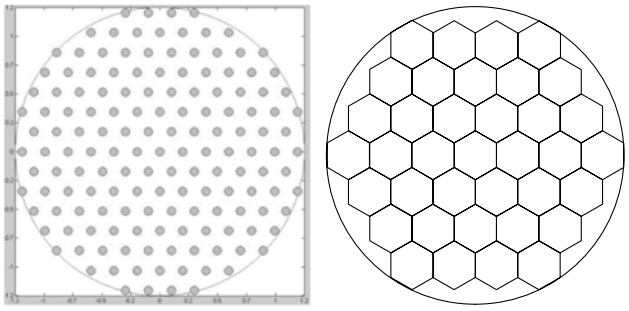

Fig. 3. Matching arrangement of the DM's actuators and the subapertures of MD-SHWFS.

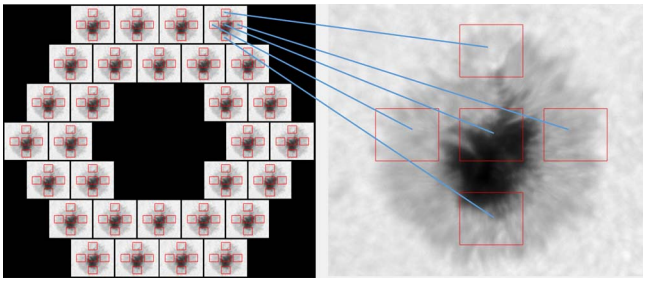

Fig. 4. Five-guide star solar MD-SHWFS arrangement of the GLAO and the corresponding areas in the far field.

is to say, if we need five guide stars, we will need five SHWFSs. For solar GLAO wavefront sensing, we can use only one MD-SHWFS to replace several SHWFSs.

Figure 4 shows the 5-guide star solar MD-SHWFS arrangement of the GLAO and the corresponding areas in the far field. The difference between the real-time controllers of the GLAO system and the AO system is that GLAO needs to compute slopes from multiple directions and averages these slopes to control the DM to get an average corrected result of the turbulence. To solve the problem of mismatch between the DM actuators and subapertures of MD-SHWFS, a modal method with 27 orders is used in our system, and the control effect is satisfactory and robust.

The main specifications of the GLAO correction loop are described as follows:

- Arrangement of subapertures: 7×7;
- Subfields in each subaperture: 5;
- FoV of each subaperture: $60'' \times 52''$ (120×104 pixels);
- FoV of each subfield: $12'' \times 10''$ (24×20 pixels);
- Frame rate of camera: 400 Hz;
- Number of the actuators of DM: 151;
- Stroke of DM: ± 2.5 μm;
- Flatted error of DM: 0.098λ PV and 0.0094λ RMS ($\lambda = 632.8$ nm).

The GLAO prototype system was integrated into the NVST and saw its first light on January 12th, 2016. Figure 5 shows the sunspot images without/with GLAO after dark- and flat-field processing.

Due to the lack of point sources on the solar surface, estimating the performance of a solar AO system is

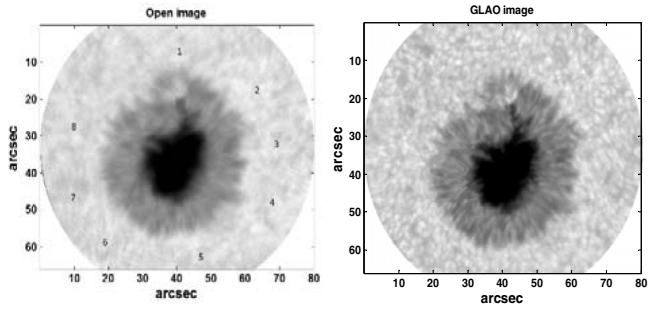

Fig. 5. Sunspot without AO (left) and with GLAO (right) closed loop for active area NOAA 12480 (705.7 at 0.6 nm).

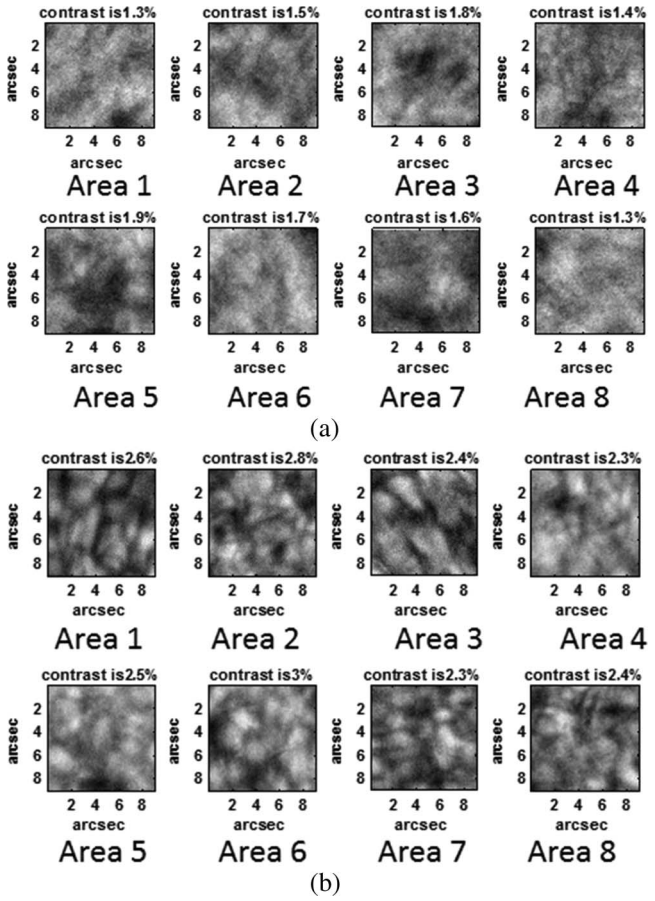

Fig. 6. Contrast of corresponding areas (a) without AO and (b) with GLAO.

generally more difficult than for stellar AO. As indicators to measure the GLAO performance, we used the contrast of the solar granulation for our evaluation. We chose eight granulation regions to compute their contrasts. The formula to calculate the granulation's contrast is defined as

$$\text{Contrast}_{\text{gra}} = \frac{(\text{image})_{\text{std}}}{(\text{image})_{\text{mean}}} \times 100\%, \tag{1}$$

where $()_{\text{std}}$ and $()_{\text{mean}}$ denote the standard deviation and arithmetic mean value of the image, respectively. Figure 6 shows the contrast of the corresponding areas. The contrasts of the eight areas before GLAO correction are 1.3%, 1.5%, 1.8%, 1.4%, 1.9%, 1.7%, 1.6%, and 1.3%, and they turn into 2.6%, 2.8%, 2.4%, 2.3%, 2.5%, 3%, 2.3%, and 2.4% after being corrected. Figure 7 shows the granulation contrast for different conditions (open loop, GLAO closed loop) in a period of time (150 images). It can be seen that the GLAO-corrected images have wider and higher contrast and reveal fine structures than those without AO. The quality of the GLAO-corrected images is noticeably improved without reaching the diffraction limit.

The solar GLAO experimental prototype is proven to be a successful application in the visible band under good seeing conditions for the 1 m NVST with a 400 Hz frame rate

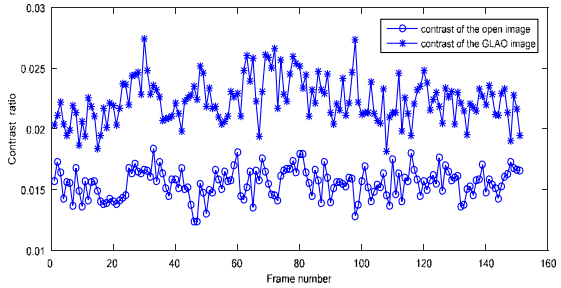

Fig. 7. Granulation contrast for open loop and GLAO closed loop in a period of time (150 images).

for low-contrast extended objects. Some technology is tested on this prototype. However, for atmospheric correction, a system with a 400 Hz framerate is too slow. In order to make the system work at the frame rate of 800 Hz, the real-time processor is optimized and upgraded, and we are waiting for the results of another experiment. Meanwhile, the improvement of our GLAO system is considered. First, based on the MD-SHWFS, the profiles of the daytime atmospheric turbulence above FSO will be tested. Second, a new MD-SHWFS will be developed with a new, larger, and faster detector to match the 151-element DM, which will make our GLAO system a practical piece of equipment.

This work was supported by the National Natural Science Foundation of China (No. 11178004) and the Laboratory Innovation Foundation of the Chinese Academy of Sciences (No. YJ15K007). We are grateful to Prof. Zhong Liu, Zhenyu Jin, and Jun Lin of Yunnan Astronomical Observatory for their help during the system setup and solar observations. Additionally, we benefited a lot from Prof. Wenhan Jiang's revision and a special acknowledgment should be given to him.

References

1. T. R. Rimmele, Proc. SPIE **4007**, 218 (2000).
2. M. Langlois, G. Moretto, K. Richards, S. Hegwer, and T. R. Rimmele, Proc. SPIE **5490**, 59 (2004).
3. T. Berkefeld, D. Soltau, and O. von der Luehe, Proc. SPIE **5903**, 59030O (2005).
4. D. Schmidt, T. Berkefeld, F. Heidecke, A. Fischer, O. von der Lühe, and D. Soltau, Proc. SPIE **9148**, 91481T (2014).
5. D. Schmidt, N. Gorceix, X. Zhang, J. Marino, R. Coulter, S. Shumko, P. Goode, T. Rimmele, and T. Berkefeld, Proc. SPIE **9148**, 91482U (2014).
6. F. Rigaut, in *European Southern Observatory Conference and Workshop Proceedings*, Vol. **58**, 11 (2002).
7. A. Kellerer, N. Gorceix, J. Marino, W. Cao, and P. R. Goode, Astron. Astrophys. **542**, A2 (2012).
8. T. R. Rimmele, F. Woeger, J. Marino, K. Richards, S. Hegwer, T. Berkefeld, D. Soltau, D. Schmidt, and T. Waldmann, Proc. SPIE **7736**, 773631 (2010).
9. D. Ren, L. Jolissaint, and X. Zhang, Publ. Astron. Soc. Pac. **127**, 469 (2015).
10. C.-H. Rao, W.-H. Jiang, C. Fang, N. Ling, W.-C. Zhou, M.-D. Ding, X.-J. Zhang, D.-H. Chen, M. Li, X.-F. Gao, and T. Mi, Chin. J. Astron. Astrophys. **3**, 576 (2003).
11. C. Rao, L. Zhu, X. Rao, C. Guan, D. Chen, S. Chen, J. Lin, and Z. Liu, Appl. Opt. **49**, G129 (2010).
12. C. Rao, L. Zhu, X. Rao, C. Guan, D. Chen, J. Lin, and Z. Liu, Chin. Opt. Lett. **8**, **966** (2010).
13. C. Rao, L. Zhu, N. Gu, X. Rao, L. Zhang, C. Guan, D. Chen, S. Chen, C. Wang, J. Lin, and Z. Liu, Proc. SPIE **8447**, 844746 (2012).
14. C. H. Rao, L. Zhu, X. J. Rao, L.-Q. Zhang, H. Bao, X.-A. Ma, N.-T. Gu, C.-L. Guan, D.-H. Chen, C. Wang, J. Lin, Z.-Y. Jin, and Z. Liu, Res. Astron. Astrophys. **16**, 23 (2016).
15. C. Rao, L. Zhu, X. Rao, L. Zhang, H. Bao, L. Kong, Y. Guo, X. Ma, M. Li, C. Wang, X. Zhang, X. Fan, D. Chen, Z. Feng, X. Wang, N. Gu, and Z. Wang, Chin. Opt. Lett. **13**, 120101 (2015).
16. Z. Liu, J. Xu, B. Z. Gu, S. Wang, J.-Q. You, L.-X. Shen, R.-W. Lu, Z.-Y. Jin, L.-F. Chen, K. Lou, Z. Li, G.-Q. Liu, Z. Xu, C.-H. Rao, Q.-Q. Hu, R.-F. Li, H.-W. Fu, F. Wang, M.-X. Bao, M.-C. Wu, and B.-R. Zhang, Res. Astron. Astrophys. **14**, 705 (2014).